
This is an electronic reprint of the original article.
This reprint may differ from the original in pagination and typographic detail.

Karki, Sabin Kumar; Ala-Laurinaho, Juha; Viikari, Ville
Integrated Metal-lens Antennas with Reduced Height at 71-76 GHz

Published in:
Proceedings of the European Conference on Antennas and Propagation

Published: 01/03/2019

Document Version
Peer-reviewed accepted author manuscript, also known as Final accepted manuscript or Post-print

Please cite the original version:
Karki, S. K., Ala-Laurinaho, J., & Viikari, V. (2019). Integrated Metal-lens Antennas with Reduced Height at 71-76 GHz. In *Proceedings of the European Conference on Antennas and Propagation* Article 8740232 (Proceedings of the European Conference on Antennas and Propagation). EurAAP Italia.
<https://ieeexplore.ieee.org/document/8740232>

This material is protected by copyright and other intellectual property rights, and duplication or sale of all or part of any of the repository collections is not permitted, except that material may be duplicated by you for your research use or educational purposes in electronic or print form. You must obtain permission for any other use. Electronic or print copies may not be offered, whether for sale or otherwise to anyone who is not an authorised user.

Integrated Metal-lens Antennas with Reduced Height at 71–76 GHz

Sabin Kumar Karki¹, Juha Ala-Laurinaho², Ville Viikari³,

¹Department of Electronics and Nanoengineering, Aalto University, Espoo, Finland, sabin.karki@aalto.fi*

²Department of Electronics and Nanoengineering, Aalto University, Espoo, Finland, juha.ala-laurinaho@aalto.fi*

³Department of Electronics and Nanoengineering, Aalto University, Espoo, Finland, ville.viikari@aalto.fi*

Abstract—A low-profile lens antenna with high efficiency is desired in many millimeter-wave applications. In this work, a new approach to integrate a dielectric lens and a metal-lens is studied to minimize the lens height. The proposed integrated metal-lens antenna minimizes the height while maintaining aperture efficiency close to that of traditional elliptical integrated lens antennas. In case of low permittivity materials, the height of the designed lens can be 35% smaller. An integrated metal-lens antenna with $8\lambda_0$ radius is designed with Teflon ($\epsilon_r = 2.1$ and $\tan\delta = 0.0002$) and $0.575\lambda_0$ parallel plate separation for operation at lower E-band, i.e., 71–76 GHz. The simulated boresight directivity of the designed lens is 32.6 dB and the peak aperture efficiency is 80%. The 3-dB gain bandwidth of the designed dual-polarized integrated metal-lens antenna is approx. 10% and the gain scan loss is 7.4 dB for beam steering range of $\pm 30^\circ$.

Index Terms— beam-steering antenna, integrated lens antenna, low-profile lens, metal-lens antenna, millimeter-wave, matching layers, square waveguides

I. INTRODUCTION

The beam focusing and steering properties of a lens antenna has made it a popular choice in the field of communications, radar, and imaging [1], [2]. The lens antennas are bulky due to the focal distance requirement for beam collimation, and therefore challenging to implement in commercial applications. Additionally, large focal distance of lens antenna increases the spillover loss [3]. Apart from the low profile requirement, the lens antennas are desired to be integrated with feed antenna to improve the mechanical rigidity and reduce the substrate modes of planar feeds and thus improving the radiation efficiency [4]. Additionally, the dual-polarized antennas are favoured in many applications.

The integrated lens antennas (ILA) are mainly implemented using homogenous dielectric materials and the focal distance is determined by the permittivity of the material used and the diameter [5]. The focal distance of a low permittivity (Teflon/HDPE) elliptical ILA is greater than the diameter and aperture efficiency is more than 90% [6], [7]. In [8], the extended hemispherical ILA designed with 1.14 f/d ratio gives approx. 80% aperture efficiency. The height of an ILA can be minimized by using high permittivity material. However, the radiation efficiency of the high permittivity ILA tends to decrease due to higher dielectric and reflection losses [9]. The multi-dielectric lens can be designed with smaller f/d ratios [10], [11]. An off-body fed sub-wavelength gradient

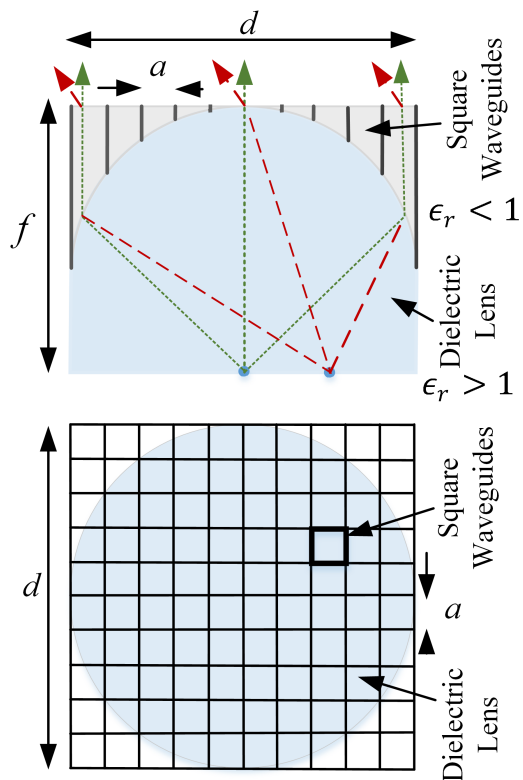


Fig. 1. Side view and top view of the integrated metal-lens antenna (I-MLA).

index lens (SUB-L) is designed with 0.5 f/d ratio [12]. The aperture efficiency of the designed SUB-L is 45%. Similarly, an integrated gradient index lens is designed with 0.25 f/d ratio [13]. However, the aperture efficiency of the lens is approx. 25%. The ILA gives maximum aperture efficiency when the focal distance is comparable with the diameter. The efforts to minimize focal distance typically leads to the degradation of aperture efficiency. Decrease in the radiation efficiency leads to increase in the lens antenna aperture or footprint in order to meet the gain requirement.

The beam focusing or collimation can also be achieved with the off-body feed metal-lens antenna (MLA) [14]. In general, the metallic plates separation distance of a MLA is kept between $0.56 - 0.6\lambda_0$ in order to obtain low effective permittivity and thus the minimum height [15], [16]. In [17],

the maximum directivity of the left side triangular notched MLA of $13\lambda_0$ diameter and variable plate separation is used at $11.8\lambda_0$ focal length. A metamaterial based MLAs with $25.5\lambda_0 \times 21\lambda_0$ aperture and $9\lambda_0$ focal length, i.e., $f/d = 0.35$, is designed, however the resulted efficiency is very low [18]. The trade-off exists between the the aperture efficiency and the height of an MLA and ILA.

Therefore, the objective of this work is to design an integrated lens antenna with reduced height as compared to the traditional ILAs. In this work, we aim to design an axis-symmetrical double lens antenna system based on dielectric lens and metal-plate lens, see Fig. 1. The designed integrated metal-lens antenna is expected to minimize the height of the lens while maintaining the high aperture efficiency. The gain, efficiency, and beam steering properties of the designed integrated MLA are compared with those of the traditionally used elliptical ILA.

The paper is organized as follows. In Section II, the integrated metal-lens antenna and its operation is described. The volumetric analysis of the HLA is presented in Section III. Section IV presents comparison between the traditional elliptical integrated lens antenna and the designed integrated MLA. Finally, in Section V conclusions and future work are discussed.

II. INTEGRATED METAL-LENS ANTENNA (I-MLA)

The operation of a dielectric ILA is based on the fact that the velocity of the wave in dielectric medium, $\epsilon_r > 1$, is slower than in vacuum, $\epsilon_r = 1$. In contrary, the phase velocity of a wave travelling through parallel plates of a MLA, $\epsilon_r < 1$, is higher as compared to vacuum. The phase velocity difference between dielectric and parallel plates can be used to achieve beam collimation in short distance. Since the collimating surface profile of a MLA and ILA are complementary to each other, a MLA and an ILA can be stacked together as shown in Fig. 1 to form an integrated metal-lens antenna (I-MLA).

The plane wave generation at the aperture of a lens is guided by the principle of equal path length [14]. The dielectric-metallic interface of the I-MLA is derived from the following equation

$$(\epsilon_r - \epsilon_m)x^2 + 2\sqrt{\epsilon_r}f(\sqrt{\epsilon_r} - \sqrt{\epsilon_m})x + \epsilon_r y^2 = 0 \quad (1)$$

where, f is the focal length, ϵ_r is the permittivity of the dielectric material and ϵ_m is the effective permittivity of the parallel plate region. The effective permittivity of the parallel plate region can be calculated using the following equation

$$\epsilon_m = 1 - \left(\frac{\lambda_0}{2a}\right)^2 \quad (2)$$

where, λ_0 is the free space wavelength and a is the separation distance between parallel plates. The relation between effective permittivity and plate separation a is also shown in Fig. 2. Ideally, $a \approx \lambda_0/2$ is desired where $\epsilon_m \approx 0$, however the

reflections from the parallel plate interface increases considerably when $a < 0.55\lambda_0$. Thus, in this study the parallel plate separation, a , range of $0.55\lambda_0 < a < \lambda_0$ is considered as there is still large variation in the ϵ_m .

In order to support dual polarization, the parallel plates are placed in both orthogonal directions with the same spacing. A square waveguide structure is formed, as shown in Fig. 1.

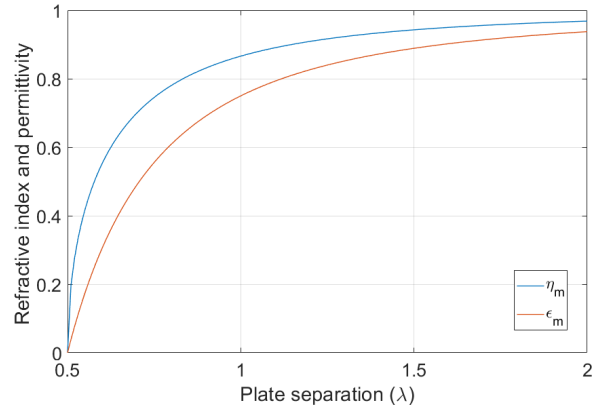


Fig. 2. Relation between the parallel plates separation a and effective permittivity ϵ_m and refractive index η_m of the medium.

III. VOLUMETRIC ANALYSIS

Fig. 3 illustrates the total height reduction of an I-MLA with respect to the permittivity of dielectric material ($4\lambda_0$ radius and $a = 0.6\lambda_0$). An elliptical ILA of same radius is taken as the reference for comparison. The figure shows that the use of parallel plates is more effective for low permittivity materials, i.e. $2 < \epsilon_r < 5$. In most of the commercial applications, the dielectric permittivity ranges between 2 to 5 due to the low loss tangent of the materials, for e.g. Teflon $\epsilon_r = 2.1$, HDPE $\epsilon_r = 2.3$, Rexolite $\epsilon_r = 2.53$, and Ultem $\epsilon_r = 3$. In case of commonly used materials like Teflon, the height of the designed I-MLA is 35.8% smaller compared to the conventional elliptical ILA. The f/d of a traditional MLA is 0.93. In case of I-MLA, the f/d varies between 0.75 and 0.6 when ϵ_r varies between 2 and 10.

The change in collimating surface profile and height of a $4\lambda_0$ I-MLA with respect to a can be seen in Fig. 4. The height of the I-MLA decreases with smaller parallel plate separation a . The height reduction is more prominent when $0.5\lambda_0 < a < 0.8\lambda_0$ as the effective permittivity changes considerably in the range. The eccentricity of the collimating surface of the lens surface decreases with decreasing a . At $a = \infty$ (air), $\epsilon_m = 1$, the eccentricity of the lens surface is $\frac{1}{\sqrt{\epsilon_r}}$ (elliptical ILA) and when $a = 0.5\lambda_0$, $\epsilon_m = 0$, then the dielectric-metallic surface has $0.5 f/d$, i.e., the surface is hemispherical.

Four I-MLAs of $4\lambda_0$ radius are designed using $0.55, 0.6, 0.7,$ and $0.8\lambda_0$ parallel plate separation and the Teflon as dielectric material. The height of the I-MLAs are $5.4, 6.0, 6.8,$ and $7.3\lambda_0$, respectively. A dielectric-filled waveguide of $2.34 \times 2.34 \text{ mm}^2$ aperture is used as feed antenna. The full-wave

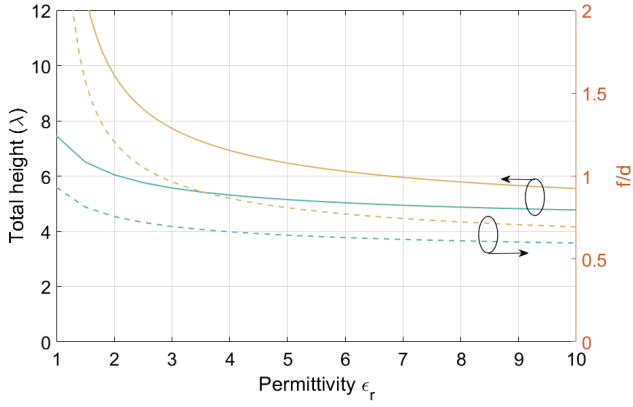


Fig. 3. Total height and f/d ratio comparison between the elliptical ILA and the I-MLA for varying material permittivity. Radius is $4\lambda_0$ and $a = 0.6\lambda_0$.

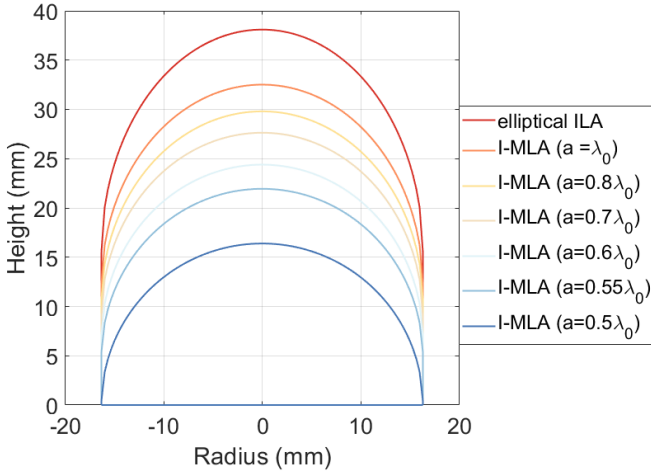


Fig. 4. Collimating surface profile of the dielectric lens and the height comparison between elliptical ILA and the I-MLA with varying plate separation. Radius of the lens is $4\lambda_0$ at 73.5 GHz. Metal-lens is not shown.

electromagnetic simulations of the designed I-MLAs are done in CST Microwave Studio. The boresight directivity variation of the I-MLAs with respect to frequency can be seen in Fig. 5. The results indicate that the boresight directivity and gain bandwidth of the I-MLA starts to decrease with smaller a . Figure 4 and 5 highlights the trade-off between the height and the gain bandwidth of a I-MLA. As a decreases, the permittivity difference in dielectric-metal interface increases which consequently leads to higher reflections. The reflected fields from dielectric-metal interface exits from the feeding plane that reduces the boresight directivity, see Fig. 6. The reflection can be minimized by introducing a quarter-wave matching layer in the dielectric-metal interface.

IV. SIMULATION COMPARISON

The topology and dimensions of the designed I-MLA are shown in Fig. 7. The I-MLA of $8\lambda_0$ diameter ($\lambda_0 = 4.078$ mm) is designed using Teflon ($\epsilon_r = 2.1$) and parallel plate separation $a = 0.575\lambda_0$ for operation in the lower E-band, i.e., 71–76 GHz. The height of the designed lens is 46.9

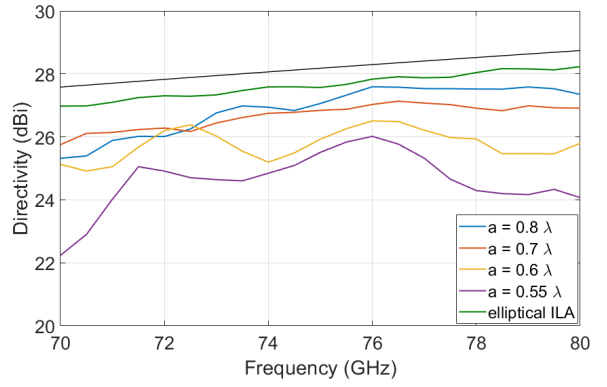


Fig. 5. Boresight directivity of a $4\lambda_0$ I-MLA with Teflon material and varying plate separation a w.r.t frequency.

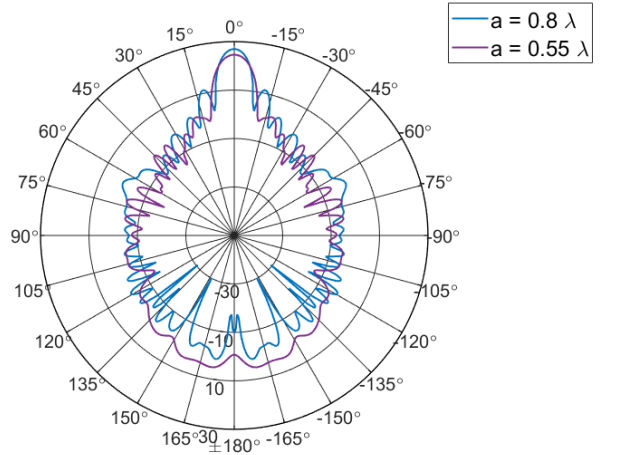


Fig. 6. Directivity radiation pattern of $4\lambda_0$ I-MLAs with Teflon material and varying plate separation.

mm. A waveguide feed with 2.34×2.34 mm² aperture is used as the feed antenna. A quarter-wave matching layer is designed to minimize the reflections from the dielectric-metallic interface. The matching layer is designed by inserting the parallel plates $\frac{\lambda_{match}}{4}$ deep inside the dielectric, where $\lambda_{match} = \frac{\lambda_0}{\sqrt{\epsilon_{match}}}$. The effective permittivity of the matching layer is $\epsilon_{match} = \sqrt{\epsilon_r} \cdot \epsilon_m = 1.34$.

The peak boresight directivity and gain of the designed I-MLA are compared with the elliptical ILA in Fig. 8. The maximum achievable directivity with uniform aperture field distribution over the given aperture area is shown in the figure by black line. The directivity of the elliptical ILA, with 1.19 f/d , is 33.35 dB and the aperture efficiency is 90%. The boresight directivity and gain of the I-MLA peaks at the designed frequency, i.e., 73.5 GHz, and the maximum directivity with and without matching layer is 32.6 dBi and 31.6 dBi, respectively, and their corresponding aperture efficiency, i.e., 80% and 60%, respectively. The 3-dB gain bandwidth of the I-MLA is approx. 7 GHz i.e. 71–78 GHz. As mentioned in previous section, the reflected fields from dielectric-metallic interface degrades the boresight directivity in case of no

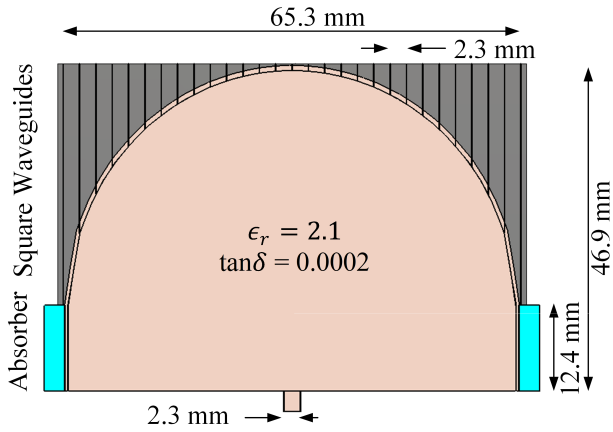


Fig. 7. Cut view of the designed $8\lambda_0$ I-MLA structure with matching layer.

matching layer. The diffraction at the edges of the metal-air surface of the I-MLA is a plausible reason for the slightly higher side lobe level at $\theta = \pm 30^\circ$, see Fig. 9.

At 74 GHz, the gain of I-MLA, 31.6 dBi, is equal to the gain of the elliptical ILA. The slightly higher aperture efficiency of the elliptical ILA is negated by high spillover and dielectric losses.

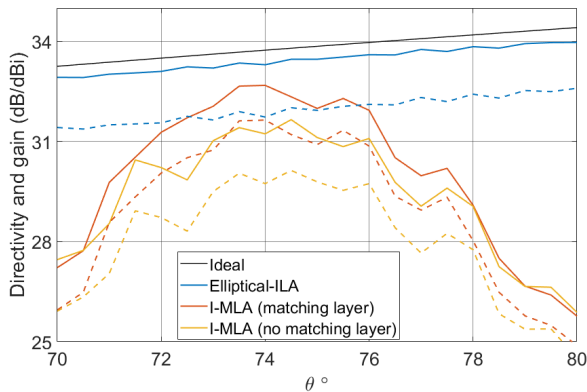


Fig. 8. Maximum gain (- -) and directivity (—) comparison of elliptical ILA and I-MLA with matching layer and without matching layer w.r.t. frequency. Lens radius is $8\lambda_0$ at 73.5 GHz.

The waveguide feed is moved to the offset positions of 4.25, 8.5, 12.75, and 16 mm to steer the beams to 8° , 16° , 24° , and 30° , respectively. In case of the elliptical ILA, the feed is moved 6, 13, 20 and 26 mm to achieved same beam steering angles. The gain radiation pattern of the steered beams are shown in the Fig. 9. The gain scan loss of the dual-polarized I-MLA is 7.4 dB for the beam steering angle of $\pm 30^\circ$, whereas the gain scan loss of the elliptical ILA is 8.46 dB for same steering range. The scan loss in I-MLA is caused by the decrease in effective area and increasing reflection at the dielectric-metallic interface with the steering angle. In addition, the increase in scan loss is also contributed by under-illumination of aperture surface in the direction opposite to feed offset.

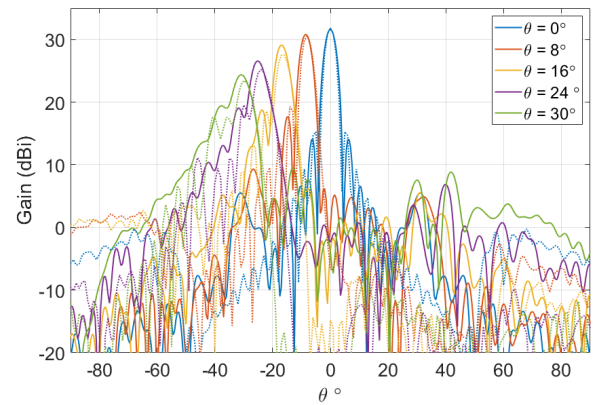


Fig. 9. Gain radiation pattern comparison between I-MLA (—) with matching layer and elliptical ILA (:) w.r.t. various beam steering angles. Lens radius is $8\lambda_0$ at 73.5 GHz.

V. CONCLUSION

An I-MLA is designed using a dielectric lens and parallel-plates. The designed I-MLA reduces the ILA height up to approx. 35% while keeping the aperture efficiency close to that of the traditional ILAs. The $8\lambda_0$ I-MLA is designed with Teflon ($\epsilon_r = 2.1$ and $\tan\delta = 0.0002$) and $0.575\lambda_0$ plate separation results in 31.6 dBi simulated boresight gain at 74 GHz. The designed I-MLA have 10% gain bandwidth and the scan loss is below 5 dB for the beam steering range of $\pm 30^\circ$.

ACKNOWLEDGMENT

The authors would like to thank Business Finland for supporting the work through 5WAVE project.

REFERENCES

- [1] J. Ala-Laurinaho, J. Aurinsalo, A. Karttunen, M. Kaunisto, A. Lamminen, J. Nurmiharju, A. V. Räsänen, J. Säily, and P. Wainio, "2-D Beam-steerable integrated lens antenna system for 5G E-band access and backhaul," *IEEE Transactions on Microwave Theory and Techniques*, vol. 64, no. 7, pp. 2244–2255, July 2016.
- [2] M. K. Saleem, H. Vettikaladi, M. A. S. Alkanhal, and M. Himdi, "Lens antenna for wide angle beam scanning at 79 GHz for automotive short range radar applications," *IEEE Transactions on Antennas and Propagation*, vol. 65, no. 4, pp. 2041–2046, April 2017.
- [3] A. Karttunen, J. Ala-Laurinaho, R. Sauleau, and A. V. Räsänen, "Reduction of internal reflections in integrated lens antennas for beam-steering," *Progress in Electromagnetics Research*, vol. 134, pp. 63–78, 2013.
- [4] G. M. Rebeiz, "Millimeter-wave and terahertz integrated circuit antennas," *Proceedings of the IEEE*, vol. 80, no. 11, pp. 1748–1770, Nov 1992.
- [5] D. F. Filipovic, S. S. Gearhart, and G. M. Rebeiz, "Double-slot antennas on extended hemispherical and elliptical silicon dielectric lenses," *IEEE Transactions on Microwave Theory and Techniques*, vol. 41, no. 10, pp. 1738–1749, Oct 1993.
- [6] S. K. Karki, J. Ala-Laurinaho, V. Viikari, and R. Valkonen, "Lens antenna design for E-band point-to-point radio links," in *2017 Progress In Electromagnetics Research Symposium - Spring (PIERS)*, May 2017, pp. 1625–1631.
- [7] A. E. I. Lamminen, S. K. Karki, A. Karttunen, M. Kaunisto, J. Säily, M. Lahdes, J. Ala-Laurinaho, and V. Viikari, "Beam-Switching Dual-Spherical Lens Antenna With Low Scan Loss at 71–76 GHz," *IEEE Antennas and Wireless Propagation Letters*, vol. 17, no. 10, pp. 1871–1875, Oct 2018.

- [8] L. Mall and R. B. Waterhouse, "Millimeter-wave proximity-coupled microstrip antenna on an extended hemispherical dielectric lens," *IEEE Transactions on Antennas and Propagation*, vol. 49, no. 12, pp. 1769–1772, Dec 2001.
- [9] S. K. Karki, A. Karttunen, J. Ala-Laurinaho, and V. Viikari, "Integrated lens antennas for E-band," in *2018 48th European Microwave Conference (EuMC)*, 2018, pp. 1–4.
- [10] C. C. Cruz, J. R. Costa, C. A. Fernandes, and S. A. Matos, "Focal-plane multibeam dual-band dielectric lens for ka-band," *IEEE Antennas and Wireless Propagation Letters*, vol. 16, pp. 432–436, 2017.
- [11] N. T. Nguyen, A. Rolland, A. V. Boriskin, G. Valerio, L. L. Coq, and R. Sauleau, "Size and weight reduction of integrated lens antennas using a cylindrical air cavity," *IEEE Transactions on Antennas and Propagation*, vol. 60, no. 12, pp. 5993–5998, Dec 2012.
- [12] A. O. Diallo, R. Czarny, B. Loiseaux, and S. Hol, "Comparison between a thin lens antenna made of structured dielectric material and conventional lens antennas, in Q-Band in a compact volume," *IEEE Antennas and Wireless Propagation Letters*, vol. 17, no. 2, pp. 307–310, Feb 2018.
- [13] M. Imbert, J. Romeu, M. Baquero-Escudero, M. Martinez-Ingles, J. Molina-Garcia-Pardo, and L. Jofre, "Assessment of LTCC-based dielectric flat lens antennas and switched-beam arrays for future 5G millimeter-wave communication systems," *IEEE Transactions on Antennas and Propagation*, vol. 65, no. 12, pp. 6453–6473, Dec 2017.
- [14] W. E. Kock, "Metal-lens antennas," *Proceedings of the IRE*, vol. 34, no. 11, pp. 828–836, Nov 1946.
- [15] G. K. Felic, E. Skafidas, and R. Evans, "Metal plate lens antenna for automotive radar at mm-wave frequencies," in *2012 6th European Conference on Antennas and Propagation (EUCAP)*, March 2012, pp. 2321–2323.
- [16] R. Mendis, M. Nagai, Y. Wang, N. Karl, and D. M. Mittleman, "Terahertz artificial dielectric lens," *Scientific reports*, vol. 6, p. 23023, 2016.
- [17] A. A. Nosich, R. Sauleau, A. Matsushima, and Y. V. Gandel, "Accurate modeling and optimization of metallic-plate waveguide lenses," in *2009 3rd European Conference on Antennas and Propagation*, March 2009, pp. 2167–2170.
- [18] V. Pacheco-Peña, B. Orazbayev, U. Beaskoetxea, M. Beruete, and M. Navarro-Cía, "Zoned near-zero refractive index fishnet lens antenna: Steering millimeter waves," *Journal of Applied Physics*, vol. 115, no. 12, p. 124902, 2014.